Spectroscopic Identification of Transitions of Fractional Rydberg States of Atomic Hydrogen

R. L. Mills,* P. Ray, B. Dhandapani, M. Nansteel, X. Chen, J. He

BlackLight Power, Inc.

493 Old Trenton Road

Cranbury, NJ 08512

ABSTRACT

Extreme ultraviolet (EUV) spectroscopy was recorded on microwave discharges of helium with 2% hydrogen. Novel emission lines were observed with energies of $q \cdot 13.6 \, eV$ where $q = 1,2,3,4,6,7,8,9, \, or \, 11$ or these lines inelastically scattered by helium atoms wherein $21.2 \, eV$ was absorbed in the excitation of $He \, (1s^2)$ to $He \, (1s^1 2p^1)$. These lines can be explained as fractional Rydberg states of atomic hydrogen. Such transitions would be extremely energetic; so, the width of the 656.2 nm Balmer α line emitted from glow discharge plasmas and the electron temperature T_e and the gas temperature of microwave plasmas were measured. The average hydrogen atom temperature of the helium-hydrogen plasma was $33\text{-}38 \, eV$ versus $\approx 3 \, eV$ for pure hydrogen. Similarly, T_e for helium-hydrogen was 28,000 K compared to 6800 K for pure helium. With a microwave input power of $40 \, W$, the thermal output power was estimated to be $238 \pm 8 \, W$ based the rise of the plasma gas temperature from room temperature to 1240 °C within 60 seconds compared to 186°C for helium alone. The corresponding power density was $24 \, MW/m^3$, and the energy balance of at least $-3 \times 10^5 \, kJ/mole \, H_2$ was high compared to the enthalpy of combustion of hydrogen of $-241.8 \, kJ/mole \, H_2$.

Key Words: hydrogen catalysis, fractional hydrogen Rydberg states, Balmer α line broadening, electron temperature

* Fax: 609-490-1066; e-mail: rmills@blacklightpower.com

I. INTRODUCTION

J. J. Balmer showed in 1885 that the frequencies for some of the lines observed in the emission spectrum of atomic hydrogen could be expressed with a completely empirical relationship. This approach was later extended by J. R. Rydberg, who showed that all of the spectral lines of atomic hydrogen were given by the equation:

$$\bar{v} = R\left(\frac{1}{n_f^2} - \frac{1}{n_i^2}\right)$$ (1)

where $R = 109,677\, cm^{-1}$, $n_f = 1,2,3,...$, $n_i = 2,3,4,...$, and $n_i > n_f$.

Niels Bohr, in 1913, developed a theory for atomic hydrogen that gave the energy levels in agreement with Rydberg's equation. An identical equation, based on a totally different theory for the hydrogen atom, was developed by E. Schrödinger, and independently by W. Heisenberg, in 1926.

$$E_n = -\frac{e^2}{n^2 8\pi\varepsilon_o a_H} = -\frac{13.598\, eV}{n^2}$$ (2a)

$$n = 1,2,3,...$$ (2b)

where a_H is the Bohr radius for the hydrogen atom ($52.947\, pm$), e is the magnitude of the charge of the electron, and ε_o is the vacuum permittivity.

The excited energy states of atomic hydrogen are given by Eq. (2a) for $n > 1$ in Eq. (2b). The $n = 1$ state is the "ground" state for "pure" photon transitions (the $n = 1$ state can absorb a photon and go to an excited electronic state, but it cannot release a photon and go to a lower-energy electronic state). However, an electron transition from the ground state to a lower-energy state may be possible by a nonradiative energy transfer such as multipole coupling or a resonant collision mechanism.

Processes that occur without photons and that require collisions are common. For example, the exothermic chemical reaction of $H + H$ to form H_2 does not occur with the emission of a photon. Rather, the reaction requires a collision with a third body, M, to remove the bond energy- $H + H + M \rightarrow H_2 + M^*$ [1]. The third body distributes the energy from the exothermic reaction, and the end result is the H_2 molecule and an

increase in the temperature of the system. Some commercial phosphors are based on nonradiative energy transfer involving multipole coupling. For example, the strong absorption strength of Sb^{3+} ions along with the efficient nonradiative transfer of excitation from Sb^{3+} to Mn^{2+}, are responsible for the strong manganese luminescence from phosphors containing these ions [2].

We propose that atomic hydrogen may undergo a catalytic reaction with certain atomized elements and ions which singly or multiply ionize at integer multiples of the potential energy of atomic hydrogen, $m \cdot 27.2\,eV$ wherein m is an integer. The theory was given previously [3-8]. The reaction involves a nonradiative energy transfer to form a hydrogen atom that is lower in energy than unreacted atomic hydrogen that corresponds to a fractional principal quantum number. That is

$$n = \frac{1}{2}, \frac{1}{3}, \frac{1}{4}, ..., \frac{1}{p}; \quad p \text{ is an integer} \tag{2c}$$

replaces the well known parameter $n = \text{integer}$ in the Rydberg equation for hydrogen excited states. The $n = 1$ state of hydrogen and the $n = \dfrac{1}{\text{integer}}$ states of hydrogen are nonradiative, but a transition between two nonradiative states is possible via a nonradiative energy transfer, say $n = 1$ to $n = 1/2$. In these cases, during the transition the electron couples to another electron transition, electron transfer reaction, or inelastic scattering reaction which can absorb the exact amount of energy that must be removed from the hydrogen atom to cause the transition. Thus, a catalyst provides a net positive enthalpy of reaction of $m \cdot 27.2\,eV$ (i.e. it absorbs $m \cdot 27.2\,eV$ where m is an integer). Certain atoms or ions serve as catalysts which resonantly accept the nonradiative energy transfer from hydrogen atoms and release the energy to the surroundings to affect electronic transitions to fractional quantum energy levels. As a consequence of the nonradiative energy transfer, the hydrogen atom becomes unstable and emits further energy until it achieves a lower-energy nonradiative state having a principal energy level given by Eqs. (2a) and (2c).

A number of independent experimental observations lead to the conclusion that atomic hydrogen can exist in fractional quantum states that are at lower energies than the traditional "ground" ($n = 1$) state. Prior

related studies that support the possibility of a novel reaction of atomic hydrogen which produces a chemically generated or assisted plasma and produces novel hydride compounds include extreme ultraviolet (EUV) spectroscopy [9-14, 17-21], characteristic emission from catalysis and the hydride ion products [11-12], lower-energy hydrogen emission [7, 9-10], plasma formation [11-14, 17-18, 20-21], Balmer α line broadening [15], anomalous plasma afterglow duration [20-21], power generation [13-17, 28], and analysis of chemical compounds [22-28]. We report that microwave and glow discharges of helium-hydrogen mixtures were studied by extreme ultraviolet (EUV) spectroscopy to search for line emission from transitions to fractional Rydberg states of atomic hydrogen. Since the electronic transitions are very energetic, Balmer α line broadening and an elevated electron temperature were anticipated and were measured. Since the second ionization energy of He^+ is an exact multiple of the potential energy of atomic hydrogen and microwave plasmas may have significant concentrations of He^+ as well as atomic hydrogen, fast kinetics observable as heat may be possible. Thus, power balances of microwave plasmas of helium-hydrogen mixtures were also measured.

II. EXPERIMENTAL

A. EUV Spectroscopy

EUV spectroscopy was recorded on hydrogen, helium, and helium-hydrogen (98/2%) microwave and glow discharge plasmas according to the methods given previously [9]. The glow discharge experimental set up was given previously [9]. The experimental set up comprising a microwave discharge gas cell light source and an EUV spectrometer which was differentially pumped is shown in Figure 1. Helium-hydrogen (98/2%) gas mixture was flowed through a half inch diameter quartz tube at 1 torr, 20 torr, or 760 torr. The gas pressure inside the cell was maintained by flowing the mixture while monitoring the pressure with a 10 torr and 1000 torr MKS Baratron absolute pressure gauge. By the same method, the hydrogen alone and helium alone plasmas were run at 20 torr. The tube was fitted with an Opthos coaxial microwave cavity

(Evenson cavity). The microwave generator was an Opthos model MPG-4M generator (Frequency: 2450 MHz). The input power to the plasma was set at 85 watts with forced air cooling of the cell.

The spectrometer was a normal incidence McPherson 0.2 meter monochromator (Model 302, Seya-Namioka type) equipped with a 1200 lines/mm holographic grating with a platinum coating. The wavelength region covered by the monochromator was $5-560 \, nm$. The EUV spectrum was recorded with a channel electron multiplier (CEM) at $2500-3000 \, V$. The wavelength resolution was about $0.02 \, nm$ (FWHM) with an entrance and exit slit width of $50 \, \mu m$. The increment was $0.2 \, nm$ and the dwell time was $500 \, ms$. Novel peak positions were based on a calibration against the known He I and He II lines.

To achieve higher sensitivity at the shorter EUV wavelengths, the light emission from a helium microwave plasma and a glow discharge plasma of a helium-hydrogen mixture (98/2%) maintained according to the methods given previously [9] were recorded with a McPherson 4° grazing incidence EUV spectrometer (Model 248/310G) equipped with a grating having 600 G/mm with a radius of curvature of $\approx 1 \, m$. The angle of incidence was 87°. The wavelength region covered by the monochromator was $5-65 \, nm$. The wavelength resolution was about $0.04 \, nm$ (FWHM) with an entrance and exit slit width of $300 \, \mu m$. A channel electron multiplier (CEM) at $2400 \, V$ was used to detect the EUV light. The increment was $0.1 \, nm$ and the dwell time was $1 \, s$.

B. Line broadening and T_e measurements

The width of the 656.2 nm Balmer α line emitted from glow discharge plasmas having atomized hydrogen from pure hydrogen alone or with a mixture of 10% hydrogen and helium at 2 torr total pressure was measured according to the methods given previously [13]. The plasmas were maintained in a cylindrical stainless steel gas cell (9.21 cm in diameter and 14.5 cm in height) with an axial hollow cathode glow discharge electrode assembly comprised a stainless steel plate (4.2 cm diameter, 0.9 mm thick) anode and a circumferential stainless steel cylindrical frame (5.1 cm OD, 7.2 cm long) perforated with evenly spaced 1 cm diameter holes. The emission was viewed normal to the cell axis

through a 1.6 mm thick UV-grade sapphire window with a 1.5 cm view diameter. The discharge was carried out under static gas conditions with a DC voltage of about 275 V which produced about 0.2 A of current. The plasma emission from the glow discharges was fiber-optically coupled through a 220F matching fiber adapter to a high resolution visible spectrometer with a resolution of $\pm 0.025\,nm$ over the spectral range $190 - 860\,nm$. The entrance and exit slits were set to $20\,\mu m$. The spectrometer was scanned between $656 - 657\,nm$ using a $0.01\,nm$ step size. The signal was recorded by a PMT with a stand alone high voltage power supply (950 V) and an acquisition controller. The data was obtained in a single accumulation with a 1 second integration time.

T_e was measured on microwave plasmas of helium alone and helium-hydrogen mixtures (90/10%) from the ratio of the intensity of the He 501.6 nm (upper quantum level n=3) line to that of the He 492.2 nm (n=4) line as described by Griem [29]. In each case, the microwave plasma cell was run under the conditions given in section A, except that the total pressure was 0.1 torr. The visible spectrum was recorded with the normal incidence EUV spectrometer as described section A except that visible spectrum $(400 - 560\,nm)$ of the cell emission was recorded with a photomultiplier tube (PMT) and a sodium salicylate scintillator. The PMT (Model R1527P, Hamamatsu) used has a spectral response in the range of $185 - 680\,nm$ with a peak efficiency at about $400\,nm$. The scan interval was $0.4\,nm$. The inlet and outlet slit were $300\,\mu m$ with a corresponding wavelength resolution of $2\,nm$. The spectra were repeated five times per experiment and were found to be reproducible within less than 5%.

C. Power balance measurements

The power balances of microwave plasmas of helium, krypton, and xenon alone and each noble gas with 5% hydrogen were determined by heat loss calorimetry [30] in the cell described in section A. A K-type thermocouple ($\pm 0.1\,°C$) housed in a stainless steel tube was placed axially inside the center of the 10 cm^3 plasma volume of the quartz microwave cell. The thermocouple was read at 0.2 second intervals with a multichannel computer data acquisition system. The gas in each case was

ultrahigh purity grade or higher. Each noble gas-hydrogen mixture (95/5%) was premixed. The gas pressure inside the cell was maintained at about 300 mtorr with a gas flow rate of 9.4 sccm that was controlled by a 0-20 sccm range mass flow controller (MKS 1179A21CS1BB) with a readout (MKS type 246). The cell pressure was monitored by a 0-10 torr MKS Baratron absolute pressure gauge.

No increase in temperature was observed when the mixture containing 5% hydrogen replaced pure krypton or xenon plasmas. In contrast, with the switch from a pure helium plasma to the mixture with 5% hydrogen at 40 W input and with forced air cooling, the quartz wall was observed to begin to melt after about 90 seconds. Whereas, the helium alone plasma run under identical conditions had a maximum temperature rise to 186 °C at 90 seconds. Thus, to achieve a higher control temperature to give greater analytical accuracy, the temperature rise of the inside of the cell was measured for 90 seconds with helium at 40 W input. The input power was stopped, and a cooling curve was measured. Then the experiment was repeated with the helium-hydrogen mixture (95/5%) run at 40 W for only 60 seconds to prevent the cell from melting. In additional controls, noncatalysts krypton or xenon replaced helium.

III. RESULTS AND DISCUSSION

A. EUV Spectroscopy

The EUV emission was recorded from microwave and glow discharge plasmas of hydrogen, helium, and helium with 2% hydrogen over the wavelength range 5-125 nm. In the case of hydrogen, no peaks were observed below 78 nm, and no spurious peaks or artifacts due to the grating or the spectrometer were observed. Only known He I and He II peaks were observed in the EUV spectra of the control helium microwave or glow discharge cell emission.

The EUV spectra (15-50 nm) of the microwave cell emission of the helium-hydrogen mixture (98/2%) that was recorded at 1, 24, and 72 hours and the helium control (dotted curve) is shown in Figure 2. Ordinary hydrogen has no emission in these regions. Novel peaks were

7

observed at 45.6 nm, 37.4 nm, and 20.5 nm which do not correspond to helium and increased with time. The pressure was increased from 20 torr to 760 torr. The peaks appeared slightly more intense at the lower pressure; so, the pressure was decreased to 1 torr and spectra were recorded.

At the 1 torr condition, additional novel peaks were observed in the short wavelength region. The short wavelength EUV spectrum (5 − 50 nm) of the control hydrogen microwave cell emission (bottom curve) is shown in Figure 3. No spectrometer artifacts were observed at the short wavelengths. The short wavelength EUV spectrum (5 − 50 nm) of the helium-hydrogen mixture (98/2%) microwave cell emission with a pressure of 1 torr (top curve) is also shown in Figure 3. Novel peaks were observed at 14.15 nm, 13.03 nm, 10.13 nm, and 8.29 nm which do not correspond to helium. It is also proposed that the 30.4 nm peak shown in Figures 2 and 3 was not entirely due to the He II transition. In the case of helium-hydrogen mixture, conspicuously absent was the 25.6 nm (48.3 eV) line of He II shown in Figure 2 which implies only a minor He II transition contribution to the 30.4 nm peak.

A novel 63.3 nm peak was observed in the EUV spectrum (50 − 65 nm) of the helium-hydrogen mixture (98/2%) glow discharge cell emission shown in Figure 4. As shown in Figures 5 and 6, the ratio of the Lβ peak to the 91.2 nm peak of the helium-hydrogen microwave plasma was 2; whereas, the ratio of the Lβ peak to the 91.2 nm peak of the control hydrogen microwave plasma was 8 which indicates that the majority of the 91.2 nm peak was due to a transition other than the binding of an electron by a proton. Based on the intensity, it is proposed that the majority of the 91.2 nm peak was due to a novel peak.

The novel peaks fit two empirical relationships. In order of energy, the set comprising the peaks at 91.2 nm, 45.6 nm, 30.4 nm, 13.03 nm, 10.13 nm, and 8.29 nm correspond to energies of $q \cdot 13.6 eV$ where $q = 1,2,3,7,9,$ or 11. In order of energy, the set comprising the peaks at 63.3 nm, 37.4 nm, 20.5 nm, and 14.15 nm correspond to energies of $q \cdot 13.6 − 21.21 eV$ where $q = 3,4,6,$ or 8. These lines can be explained as electronic transitions to fractional Rydberg states of atomic hydrogen given by Eqs. (2a) and (2c) wherein the catalytic system involves helium ions because the second ionization energy of helium is 54.417 eV, which is equivalent to $2 \cdot 27.2 eV$. In this

case, the catalysis reaction is

$$54.417 \, eV + He^+ + H[a_H] \rightarrow He^{2+} + e^- + H\left[\frac{a_H}{3}\right] + 108.8 \, eV \tag{3}$$

$$He^{2+} + e^- \rightarrow He^+ + 54.417 \, eV \tag{4}$$

And, the overall reaction is

$$H[a_H] \rightarrow H\left[\frac{a_H}{3}\right] + 54.4 \, eV + 54.4 \, eV \tag{5}$$

Since the products of the catalysis reaction have binding energies of $m \cdot 27.2 \, eV$, they may further serve as catalysts. Thus, further catalytic transitions may occur: $n = \frac{1}{3} \rightarrow \frac{1}{4}, \frac{1}{4} \rightarrow \frac{1}{5}$, and so on.

Electronic transitions to Rydberg states given by Eqs. (2a) and (2c) catalyzed by the resonant nonradiative transfer of $m \cdot 27.2 \, eV$ would give rise to a series of emission lines of energies $q \cdot 13.6 \, eV$ where q is an integer. It is further proposed that the photons that arise from hydrogen transitions may undergo inelastic helium scattering. That is, the catalytic reaction

$$H[a_H] \xrightarrow{\ He^+\ } H\left[\frac{a_H}{3}\right] + 54.4 \, eV + 54.4 \, eV \tag{6}$$

yields two $54.4 \, eV$ photons ($22.8 \, nm$). When each of these photons strikes $He \, (1s^2)$, $21.2 \, eV$ is absorbed in the excitation to $He \, (1s^1 2p^1)$. This leaves a $33.19 \, eV$ ($37.4 \, nm$) photon peak and a $21.2 \, eV$ ($58.4 \, nm$) photon from $He \, (1s^1 2p^1)$. Thus, for helium the inelastic scattered peak of $54.4 \, eV$ photons from Eq. (3) is given by

$$E = 54.4 \, eV - 21.21 \, eV = 33.19 \, eV \ (37.4 \, nm) \tag{7}$$

A novel peak shown in Figures 2 and 3 was observed at $37.4 \, nm$. Furthermore, the intensity of the $58.4 \, nm$ shown in Figure 4 was off-scale with 56,771 photons/sec. Thus, the transition $He \, (1s^2) \rightarrow He \, (1s^1 2p^1)$ dominated the inelastic scattering of EUV peaks. The general reaction is

$$photon \, (h\nu) + He \, (1s^2) \rightarrow He \, (1s^1 2p^1) + photon \, (h\nu - 21.21 \, eV) \tag{8}$$

With Eq. (8), the two empirical series may be combined. The energies for the novel lines in order of energy are $13.6 \, eV$, $27.2 \, eV$, $40.8 \, eV$, $54.4 \, eV$, $81.6 \, eV$, $95.2 \, eV$, $108.8 \, eV$, $122.4 \, eV$ and $149.6 \, eV$. The corresponding peaks are $91.2 \, nm$, $45.6 \, nm$, $30.4 \, nm$ with $63.3 \, nm$, $37.4 \, nm$, $20.5 \, nm$, $13.03 \, nm$, $14.15 \, nm$, $10.13 \, nm$, and $8.29 \, nm$, respectively. Thus, the identified novel lines correspond to energies of $q \cdot 13.6 \, eV$ where $q = 1, 2, 3, 4, 6, 7, 8, 9, \, or \, 11$ or these lines inelastically scattered by helium atoms wherein $21.2 \, eV$ was

absorbed in the excitation of $He(1s^2)$ to $He(1s^12p^1)$. There is remarkable agreement between the data and the proposed transitions to fractional Rydberg states and these lines inelastically scattered by helium according to Eq. (8). All other peaks could be assigned to He I, He II, second order lines, or atomic or molecular hydrogen emission. No known lines of helium or hydrogen explain the $q \cdot 13.6 \, eV$ related set of peaks. Given that these spectra are readily repeatable, these peaks may have been overlooked in the past without considering the role of the helium scattering. It is also remarkable that the novel lines are moderately intense based on the low grating efficiency at these short wavelengths.

B. Line broadening and T_e measurements

The results of the 656.2 nm Balmer α line width measured with a high resolution ($\pm 0.025 \, nm$) visible spectrometer on glow discharge plasmas having atomized hydrogen from pure hydrogen alone and helium-hydrogen (90/10%) is given in Figure 7. Using the method of Kuraica and Konjevic [31] and Videnocic et al. [32], the energetic hydrogen atom densities and energies were calculated. It was found that helium-hydrogen showed significant broadening corresponding to an average hydrogen atom temperature of $33\text{-}38 \, eV$ and an atom density of $3 \times 10^{13} \, atoms/cm^3$; whereas, pure hydrogen showed no excessive broadening corresponding to an average hydrogen atom temperature of $\approx 3 \, eV$ and an atom density of only $5 \times 10^{13} \, atoms/cm^3$ even though 10 times more hydrogen was present. Similarly, the average electron temperature for helium-hydrogen microwave plasma was 28,000 K; whereas, the corresponding temperature of helium alone was only 6800 K.

C. Power balance measurements

Since a significant increase in ion and electron temperature was observed with helium-hydrogen discharge and microwave plasmas, respectively, and energetic hydrino lines were observed at short wavelengths in the corresponding microwave plasmas that required a very significant reaction rate due to low photon detection efficiency in this region, the power balance was measured on the helium-hydrogen

microwave plasmas by heat loss calorimetry [30]. No increase in temperature with the addition of hydrogen to krypton or xenon was observed. In contrast, a remarkable temperature increase was observed when hydrogen was added to the helium microwave plasma. The temperature rise as a function of time for helium alone and the helium-hydrogen mixture (95/5%) is shown in Figure 8. The microwave input power to the helium alone and the helium-hydrogen mixture was set at 40 W. The constant microwave input was maintained for 60 seconds and 90 seconds, respectively, and then terminated. The cooling curves were then recorded.

The power balance was determined by modeling the heat flow from the quartz reactor wherein the parameters of the model were taken from the Newton cooling curves. Consider a small heat increment

$$dQ_t = P_{out}dt = dQ_m + dQ_l = CdT_h - CdT_c \qquad (9)$$

where Q_t is the total heat, Q_m is the measured heat, Q_l is the lost heat, P_{out} is the power output, t is time, C is the system heat capacity, dT_h is the temperature rise due to heating, and dT_c is the temperature drop due to cooling (dT_c is negative). The system heat capacity is a function of temperature, and at a given temperature, the power output can be expressed by the following equation,

$$P_{out} = C\left(\frac{dT_h}{dt} - \frac{dT_c}{dt}\right) \qquad (10)$$

The slopes dT_h/dt and dT_c/dt can be calculated from the heating and cooling curves, respectively. Assuming that, at a given temperature, the heat capacities of the two systems (system 1: helium alone; system 2: helium-hydrogen) are the same, $C_1 = C_2$, then the power ratio can be calculated by

$$R = \frac{P_{out,2}}{P_{out,1}} = \frac{\left(\dfrac{dT_{h,2}}{dt} - \dfrac{dT_{c,2}}{dt}\right)}{\left(\dfrac{dT_{h,1}}{dt} - \dfrac{dT_{c,1}}{dt}\right)} \qquad (11)$$

The slopes of the heating and cooling curves were calculated using the experimental data presented in Figure 8. The power ratios were calculated by Eq. (11) in the temperature range $\Delta T = 50 - 150\,°C$, where ΔT was the difference between the plasma temperature and the room temperature, 24 °C. The following power balance existed in the

11

microwave plasma systems,

$$P_{out} = P_{in} + P_{ex}$$ (12)

where P_{in} was the input power and P_{ex} was the excess power. For the helium plasma, there was no excess power, $P_{ex,1} = 0$, $P_{out,1} = P_{in,1} = 40\ W$.

The calculated results are given in Table 1. The average power ratio is $R = 5.94$ with a standard deviation of 0.21. Since the temperature was recorded at 200 millisecond intervals, the data in Figure 8 shows that the temperature rise as a function of time was variable over the 60 second reaction time and significantly accelerated at temperatures above those used in the power balance determination based on Eq. (11). Thus, the analysis shown in Table 1 is conservative.

The reactor volume was $10\ cm^3$, and the hydrogen flow rate was 0.5 sccm. Therefore, with a microwave input power of $40\ W$, the thermal output power was measured to be $238 \pm 8\ W$ corresponding to a plasma gas temperature rise from room temperature to 1240 °C within 60 seconds, an unoptimized gain of about 6 times the input power, an excess power of $198 \pm 8\ W$, a power density of $24\ MW/m^3$, and an energy balance of at least $-3 \times 10^5\ kJ/mole\ H_2$ compared to the enthalpy of combustion of hydrogen of $-241.8\ kJ/mole\ H_2$.

IV. CONCLUSION

We report that extreme ultraviolet (EUV) spectroscopy was recorded on microwave and glow discharges of helium with 2% hydrogen. Novel emission lines were observed with energies of $q \cdot 13.6\ eV$ where $q = 1,2,3,4,6,7,8,9,\ or\ 11$ or these lines inelastically scattered by helium atoms wherein $21.2\ eV$ was absorbed in the excitation of $He\ (1s^2)$ to $He\ (1s^1 2p^1)$. These lines were identified as transitions to fractional Rydberg states of atomic hydrogen. In glow discharge plasmas, an average hydrogen atom temperature of $33-38\ eV$ was observed by line broadening with the presence of helium ion catalyst with hydrogen; whereas, pure hydrogen plasmas showed no excessive broadening corresponding to an average hydrogen atom temperature of $\approx 3\ eV$. Similarly, the average electron temperature for helium-hydrogen microwave plasmas was 28,000 K; whereas, the corresponding temperature of helium alone was only 6800 K.

Excess thermal power of about 240 W and a gain of 6 was observed from helium-hydrogen microwave plasmas. The power from the catalytic reaction of helium ions with atomic hydrogen corresponded to a volumetric power density of over $24\,MW/m^3$ which is about 100 times that of many coal fired electric power plants, and rivals some internal combustion engines. In addition, the presently observed and previously reported energy balances [15-16] were over $100\,eV/H\,atom$ which matched the present and previously reported EUV emission that corresponded to over $100\,eV/H\,atom$ [9-11, 19]. Since the net enthalpy released is at least 100 times that of combustion, the catalysis of atomic hydrogen represents a new source of energy with H_2O as the source of hydrogen fuel. Moreover, rather that air pollutants or radioactive waste, novel hydride compounds with potential commercial applications are the products [21-28]. Since the power is in the form of a plasma that may form at room temperature, high-efficiency, low cost direct energy conversion may be possible, thus, avoiding heat engines such as turbines and the severe limitations of fuel cells [33-35]. Significantly lower capital costs and lower commercial operating costs than that of any known competing energy source are anticipated.

ACKNOWLEDGMENT

REFERENCES

1. N. V. Sidgwick, *The Chemical Elements and Their Compounds*, Volume I, Oxford, Clarendon Press, (1950), p.17.
2. M. D. Lamb, *Luminescence Spectroscopy*, Academic Press, London, (1978), p. 68.
3. R. Mills, *The Grand Unified Theory of Classical Quantum Mechanics*, September 2001 Edition, BlackLight Power, Inc., Cranbury, New Jersey, Distributed by Amazon.com; posted at www.blacklightpower.com.
4. R. Mills, "The Grand Unified Theory of Classical Quantum Mechanics", Global Foundation, Inc. Orbis Scientiae entitled *The Role of Attractive and Repulsive Gravitational Forces in Cosmic Acceleration of Particles*

The Origin of the Cosmic Gamma Ray Bursts, (29th Conference on High Energy Physics and Cosmology Since 1964) Dr. Behram N. Kursunoglu, Chairman, December 14-17, 2000, Lago Mar Resort, Fort Lauderdale, FL.

5. R. Mills, "The Grand Unified Theory of Classical Quantum Mechanics", Global Foundation, Inc. Orbis Scientiae entitled *The Role of Attractive and Repulsive Gravitational Forces in Cosmic Acceleration of Particles The Origin of the Cosmic Gamma Ray Bursts*, (29th Conference on High Energy Physics and Cosmology Since 1964) Dr. Behram N. Kursunoglu, Chairman, December 14-17, 2000, Lago Mar Resort, Fort Lauderdale, FL, Kluwer Academic/Plenum Publishers, New York, pp. 243-258.

6. R. Mills, "The Grand Unified Theory of Classical Quantum Mechanics", Int. J. of Hydrogen Energy, in press.

7. R. Mills, "The Hydrogen Atom Revisited", Int. J. of Hydrogen Energy, Vol. 25, Issue 12, December, (2000), pp. 1171-1183.

8. R. Mills, The Nature of Free Electrons in Superfluid Helium--a Test of Quantum Mechanics and a Basis to Review its Foundations and Make a Comparison to Classical Theory, Int. J. Hydrogen Energy, Vol. 26, No. 10, (2001), pp. 1059-1096.

9. R. Mills, P. Ray, "Spectral Emission of Fractional Quantum Energy Levels of Atomic Hydrogen from a Helium-Hydrogen Plasma and the Implications for Dark Matter", Int. J. Hydrogen Energy, in press.

10. R. Mills, P. Ray, "Vibrational Spectral Emission of Fractional-Principal-Quantum-Energy-Level Hydrogen Molecular Ion", Int. J. Hydrogen Energy, in press.

11. R. Mills, P. Ray, Spectroscopic Identification of a Novel Catalytic Reaction of Potassium and Atomic Hydrogen and the Hydride Ion Product, Int. J. Hydrogen Energy, Vol. 27, No. 2, December, (2001), pp. 183-192.

12. R. Mills, "Spectroscopic Identification of a Novel Catalytic Reaction of Atomic Hydrogen and the Hydride Ion Product", Int. J. Hydrogen Energy, Vol. 26, No. 10, (2001), pp. 1041-1058.

13. R. Mills and M. Nansteel, "Argon-Hydrogen-Strontium Plasma Light Source", IEEE Transactions on Plasma Science, submitted.

14. R. Mills, M. Nansteel, and Y. Lu, "Excessively Bright Hydrogen-Strontium Plasma Light Source Due to Energy Resonance of Strontium

with Hydrogen", European Journal of Physics D, submitted.

15. R. Mills, A. Voigt, P. Ray, M. Nanstell, "Measurement of Hydrogen Balmer Line Broadening and Thermal Power Balances of Noble Gas-Hydrogen Discharge Plasmas", Int. J. Hydrogen Energy, in press.

16. R. Mills, N. Greenig, S. Hicks, "Optically Measured Power Balances of Anomalous Discharges of Mixtures of Argon, Hydrogen, and Potassium, Rubidium, Cesium, or Strontium Vapor", Int. J. Hydrogen Energy, in press.

17. R. Mills, M. Nansteel, and Y. Lu, "Observation of Extreme Ultraviolet Hydrogen Emission from Incandescently Heated Hydrogen Gas with Strontium that Produced an Anomalous Optically Measured Power Balance", Int. J. Hydrogen Energy, Vol. 26, No. 4, (2001), pp. 309-326.

18. R. Mills, J. Dong, Y. Lu, "Observation of Extreme Ultraviolet Hydrogen Emission from Incandescently Heated Hydrogen Gas with Certain Catalysts", Int. J. Hydrogen Energy, Vol. 25, (2000), pp. 919-943.

19. R. Mills, "Observation of Extreme Ultraviolet Emission from Hydrogen-KI Plasmas Produced by a Hollow Cathode Discharge", Int. J. Hydrogen Energy, Vol. 26, No. 6, (2001), pp. 579-592.

20. R. Mills, "Temporal Behavior of Light-Emission in the Visible Spectral Range from a Ti-K2CO3-H-Cell", Int. J. Hydrogen Energy, Vol. 26, No. 4, (2001), pp. 327-332.

21. R. Mills, T. Onuma, and Y. Lu, "Formation of a Hydrogen Plasma from an Incandescently Heated Hydrogen-Catalyst Gas Mixture with an Anomalous Afterglow Duration", Int. J. Hydrogen Energy, Vol. 26, No. 7, July, (2001), pp. 749-762.

22. R. Mills, B. Dhandapani, M. Nansteel, J. He, A. Voigt, "Identification of Compounds Containing Novel Hydride Ions by Nuclear Magnetic Resonance Spectroscopy", Int. J. Hydrogen Energy, Vol. 26, No. 9, Sept. (2001), pp. 965-979.

23. R. Mills, B. Dhandapani, N. Greenig, J. He, "Synthesis and Characterization of Potassium Iodo Hydride", Int. J. of Hydrogen Energy, Vol. 25, Issue 12, December, (2000), pp. 1185-1203.

24. R. Mills, "Novel Inorganic Hydride", Int. J. of Hydrogen Energy, Vol. 25, (2000), pp. 669-683.

25. R. Mills, "Novel Hydrogen Compounds from a Potassium Carbonate Electrolytic Cell", Fusion Technology, Vol. 37, No. 2, March, (2000), pp.

157-182.

26. R. Mills, B. Dhandapani, M. Nansteel, J. He, T. Shannon, A. Echezuria, "Synthesis and Characterization of Novel Hydride Compounds", Int. J. of Hydrogen Energy, Vol. 26, No. 4, (2001), pp. 339-367.

27. R. Mills, "Highly Stable Novel Inorganic Hydrides", Journal of New Materials for Electrochemical Systems, in press.

28. R. Mills, W. Good, A. Voigt, Jinquan Dong, "Minimum Heat of Formation of Potassium Iodo Hydride", Int. J. Hydrogen Energy, Vol. 26, No. 11, Oct., (2001), pp. 1199-1208.

29. H. R. Griem, *Principle of Plasma Spectroscopy*, Cambridge University Press, (1987).

30. C. Chen, T. Wei, L. R. Collins, and J. Phillips, "Modeling the discharge region of a microwave generated hydrogen plasma", J. Phys. D: Appl. Phys., Vol. 32, (1999), pp. 688-698.

31. M. Kuraica, N. Konjevic, "Line shapes of atomic hydrogen in a plane-cathode abnormal glow discharge", Physical Review A, Volume 46, No. 7, October (1992), pp. 4429-4432.

32. I. R. Videnocic, N. Konjevic, M. M. Kuraica, "Spectroscopic investigations of a cathode fall region of the Grimm-type glow discharge", Spectrochimica Acta, Part B, Vol. 51, (1996), pp. 1707-1731.

33. R. Mills, "BlackLight Power Technology-A New Clean Hydrogen Energy Source with the Potential for Direct Conversion to Electricity", Proceedings of the National Hydrogen Association, 12 th Annual U.S. Hydrogen Meeting and Exposition, *Hydrogen: The Common Thread*, The Washington Hilton and Towers, Washington DC, (March 6-8, 2001), pp. 671-697.

34. R. Mills, "BlackLight Power Technology-A New Clean Energy Source with the Potential for Direct Conversion to Electricity", Global Foundation International Conference on "Global Warming and Energy Policy", Dr. Behram N. Kursunoglu, Chairman, Fort Lauderdale, FL, November 26-28, 2000, Kluwer Academic/Plenum Publishers, New York, pp. 1059-1096.

35. R. Mayo, R. Mills, M. Nansteel, "On the Potential of Direct and MHD Conversion of Power from a Novel Plasma Source to Electricity for Microdistributed Power Applications", IEEE Transactions on Plasma

16

Science, submitted.

Table 1. Calculation of Power Ratios between Helium-Hydrogen and Helium Plasmas.

ΔT (°C)	$dT_{h,1}/dt$ (°C/sec)	$dT_{c,1}/dt$ (°C/sec)	$dT_{h,2}/dt$ (°C/sec)	$dT_{c,2}/dt$ (°C/sec)	Power Ratio, R
40	4.43	-1.00	29.14	-1.16	5.59
50	3.76	-1.21	28.91	-1.35	6.10
60	3.42	-1.45	28.67	-1.57	6.21
70	3.20	-1.72	28.44	-1.81	6.14
80	3.01	-2.02	28.22	-2.07	6.03
90	2.77	-2.32	27.99	-2.34	5.95
100	2.48	-2.63	27.77	-2.60	5.94
110	2.14	-2.94	27.56	-2.84	5.99
120	1.78	-3.28	27.34	-3.06	6.00
130	1.44	-3.72	27.13	-3.25	5.88
140	1.15	-4.39	26.93	-3.41	5.47

Figure Captions

Figure 1. The experimental set up comprising a microwave discharge gas cell light source and an EUV spectrometer which was differentially pumped.

Figure 2. The EUV spectra (15-50 nm) of the microwave cell emission of the helium-hydrogen mixture (98/2%) recorded at 1, 24, and 72 hours with a normal incidence EUV spectrometer and a CEM, and control helium (dotted curve) recorded with a 4° grazing incidence EUV spectrometer and a CEM. The pressure was maintained at 20 torr. Only known He I and He II peaks were observed with the helium control. Reproducible novel emission lines that increased with time were observed at 45.6 nm and 30.4 nm with energies of $q \cdot 13.6 \, eV$ where $q = 2 \, or \, 3$ and at 37.4 nm and 20.5 nm with energies of $q \cdot 13.6 \, eV$ where $q = 4 \, or \, 6$ that were inelastically scattered by helium atoms wherein $21.2 \, eV$ (58.4 nm) was absorbed in the excitation of $He \, (1s^2)$.

Figure 3. The short wavelength EUV spectra (5-50 nm) of the microwave cell emission of the helium-hydrogen mixture (98/2%) (top curve) and the control hydrogen (bottom curve) recorded with a normal incidence EUV spectrometer and a CEM. No hydrogen emission was observed in this region, and no instrument artifacts were observed. Reproducible novel emission lines were observed at 45.6 nm, 30.4 nm, 13.03 nm, 10.13 nm, and 8.29 nm with energies of $q \cdot 13.6 \, eV$ where $q = 2,3,7,9, \, or \, 11$ and at 37.4 nm, 20.5 nm, and 14.15 nm with energies of $q \cdot 13.6 \, eV$ where $q = 4,6, \, or \, 8$ that were inelastically scattered by helium atoms wherein $21.2 \, eV$ (58.4 nm) was absorbed in the excitation of $He \, (1s^2)$.

Figure 4. The EUV spectrum (50-65 nm) of the helium-hydrogen mixture (98/2%) glow discharge cell emission recorded with a 4° grazing incidence EUV spectrometer and a CEM. The pressure was maintained at 400 mtorr. A novel line was observed at 63.3 nm corresponding to the 30.4 nm fractional Rydberg state transition shown in Figures 2 and 3 that was inelastically scattered by helium atoms wherein $21.2 \, eV$ (58.4 nm) was absorbed in the excitation of $He \, (1s^2)$.

Figure 5. The EUV spectrum (88-125 nm) of the helium-hydrogen mixture (98/2%) microwave cell emission recorded with a normal incidence EUV spectrometer and a CEM. The pressure was maintained at
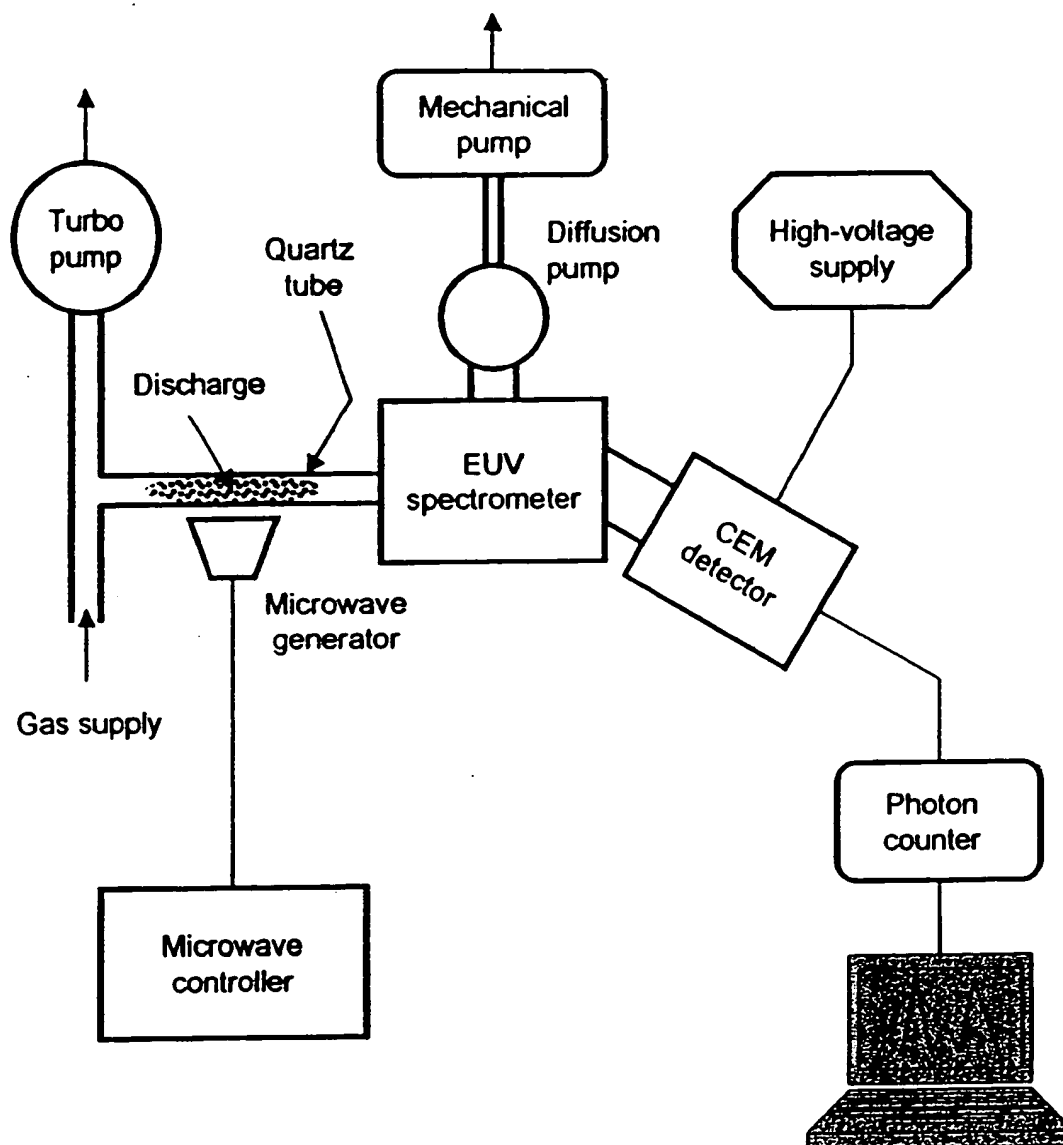
20 torr. An emission line was observed at 91.2 nm with an energy of $q \cdot 13.6 \, eV$ where $q = 1$ which was identified as a fractional Rydberg state transition based on the 91.2 nm line intensity relative to Lβ compared to that of the control hydrogen plasma.

Figure 6. The EUV spectrum (80–108 nm) of the control hydrogen microwave discharge cell emission recorded with a normal incidence EUV spectrometer and a CEM.

Figure 7. The 656.2 nm Balmer α line width recorded with a high resolution (±0.025 nm) visible spectrometer on a helium-hydrogen mixture (90/10%) discharge plasma. Significant broadening was observed corresponding to an average hydrogen atom temperature of 33-38 eV.

Figure 8. The temperature rise as a function of time for helium alone and the helium-hydrogen mixture (95/5%) with microwave input power set at 40 W. The constant microwave input was maintained for 90 seconds and 60 seconds, respectively, and then terminated. The cooling curves were then recorded. The maximum temperature of the helium-hydrogen mixture plasma and helium alone plasma was 1240°C and 186°C, respectively. The thermal output power of the helium-hydrogen plasma was determined to be 240 W.

Fig. 1

Turbo pump

Quartz tube

Discharge

Mechanical pump

Diffusion pump

High-voltage supply

EUV spectrometer

CEM detector

Microwave generator

Gas supply

Microwave controller

Photon counter

Fig. 2

Photon Counts/sec

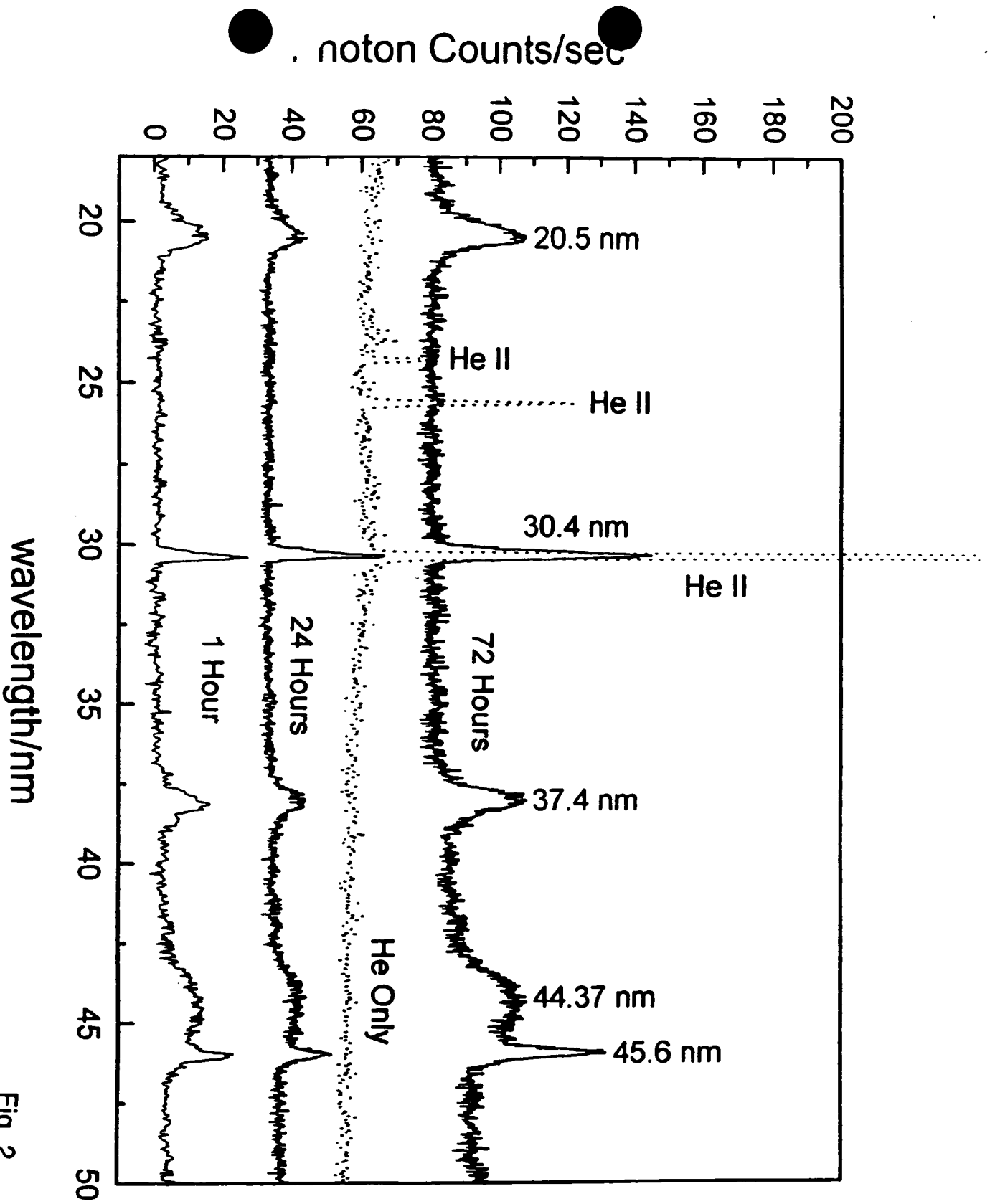20.5 nm

He II

He II

30.4 nm

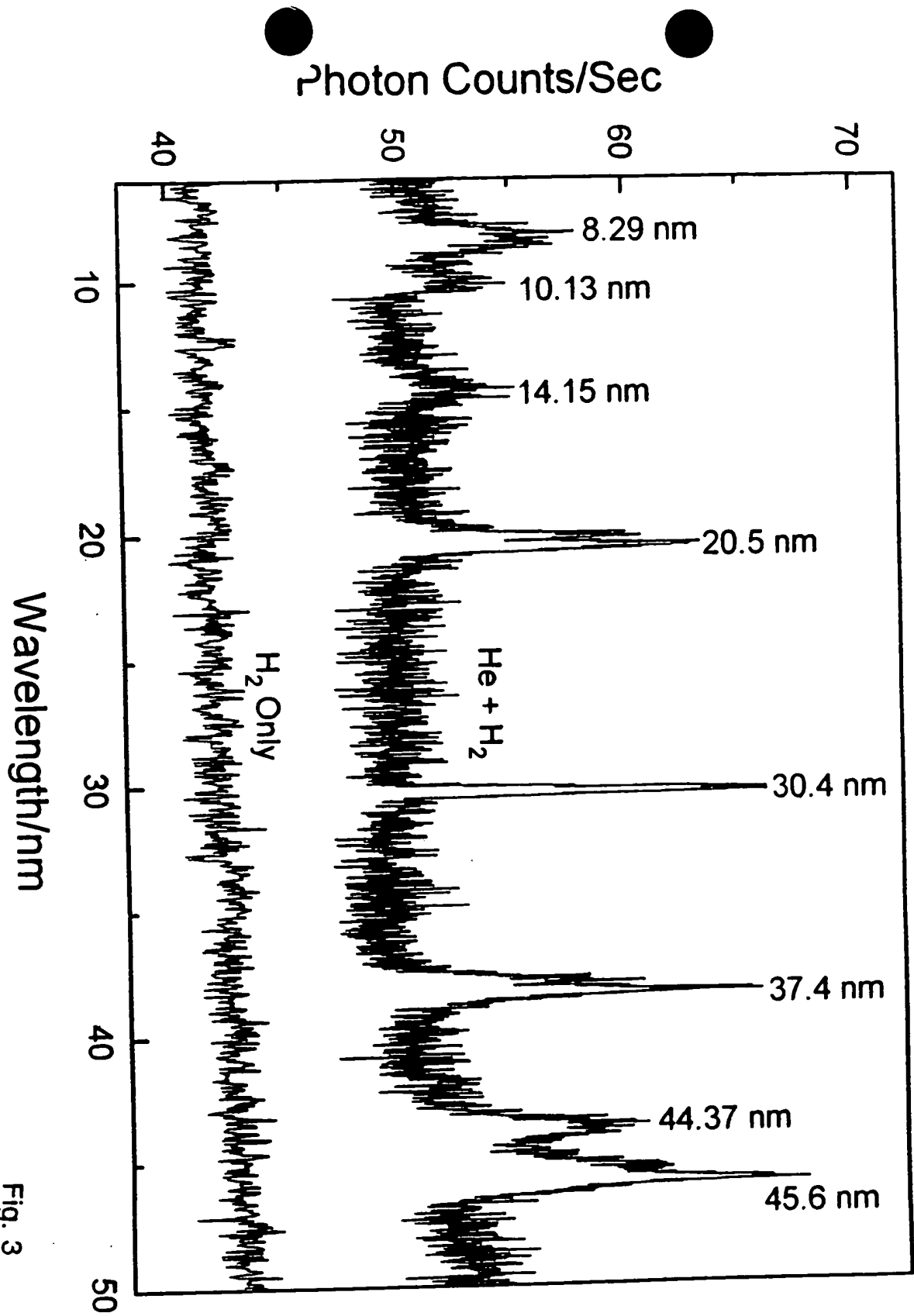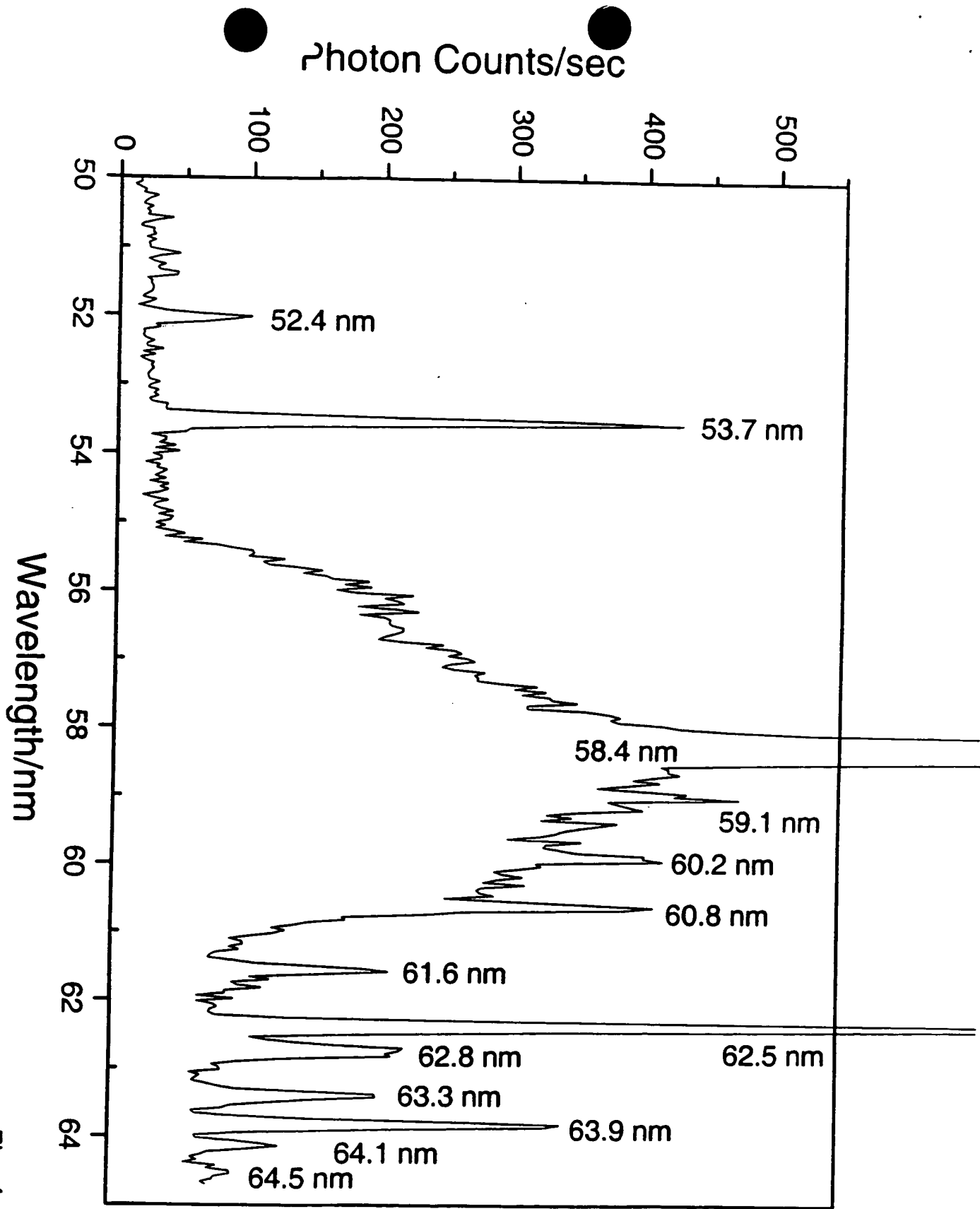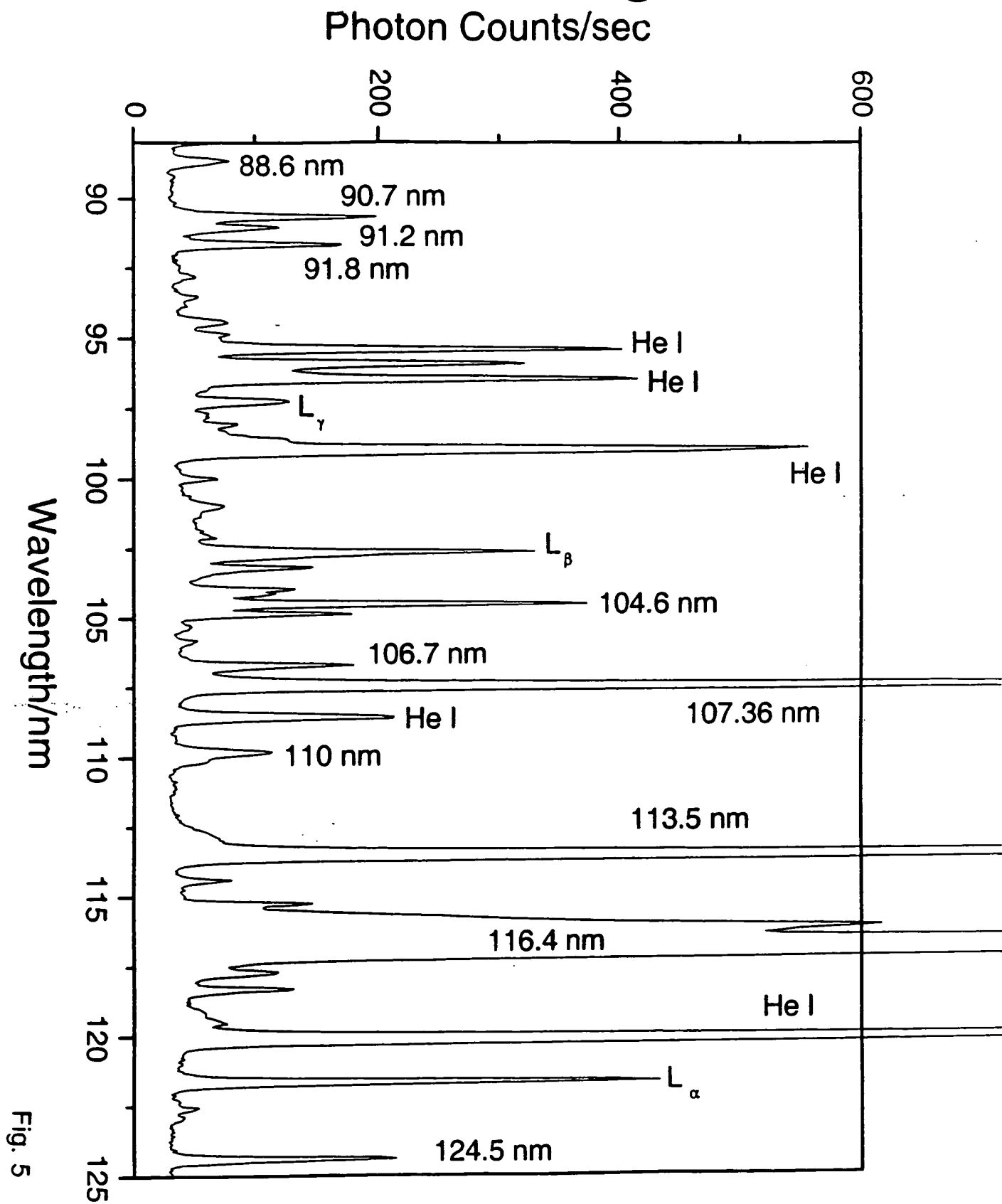He II

37.4 nm

44.37 nm

45.6 nm

1 Hour

24 Hours

He Only

72 Hours

wavelength/nm

Fig. 3

Fig. 4

Fig. 5

Fig. 6

Fig. 7

Fig. 8

Temperature/°C

He at 40 watts

He/H$_2$ at 40 watts

Time/min